



VICTORIA UNIVERSITY
MELBOURNE AUSTRALIA

Alterations in dihydropyridine receptors in dystrophin-deficient cardiac muscle

This is the Accepted version of the following publication

Woolf, PJ, Lu, Sai, Cornford-Nairn, R, Watson, M, Xiao, XH, Holroyd, SM, Brown, Lindsay and Hoey, Andrew (2006) Alterations in dihydropyridine receptors in dystrophin-deficient cardiac muscle. *American Journal of Physiology - Heart and Circulatory Physiology*, 290 (6). H2439-H2445. ISSN 0363-6135

The publisher's official version can be found at
<https://www.physiology.org/doi/full/10.1152/ajpheart.00844.2005>
Note that access to this version may require subscription.

Downloaded from VU Research Repository <https://vuir.vu.edu.au/39715/>

Abstract

The deficiency of dystrophin, a critical membrane stabilising protein, in the *mdx* mouse causes an elevation in intracellular calcium in myocytes. One mechanism that could elicit increases in intracellular calcium is enhanced influx via the L-type calcium channels. This study investigated the effects of the dihydropyridines BayK 8644 and nifedipine and alterations in dihydropyridine receptors in dystrophin-deficient *mdx* hearts. A lower force of contraction and a reduced potency of extracellular calcium ($P<0.05$) was evident in *mdx* left atria. The dihydropyridine agonist Bay K 8644 and antagonist nifedipine had 2.7 and 1.9 fold lower potencies in contracting left atria ($P<0.05$). This corresponded with a 2.0 fold reduction in dihydropyridine receptor affinity evident from radioligand binding studies of *mdx* ventricular homogenates ($P<0.05$). Increased ventricular dihydropyridine receptor protein was evident from both radioligand binding studies and Western blots and was accompanied by increased mRNA levels ($P<0.05$). Patch clamp studies in isolated ventricular myocytes showed no change in L-type calcium current density, but revealed delayed channel inactivation ($P<0.05$). This study indicates that a deficiency of dystrophin leads to changes in dihydropyridine receptors and L-type calcium channel properties that may contribute to enhanced calcium influx. Increased influx is a potential mechanism for the calcium overload observed in dystrophin deficient cardiac muscle.

Keywords:

Duchenne muscular dystrophy; calcium channels, heart

Introduction

Dystrophin is an integral subsarcolemmal protein essential for stabilising both the dystrophin associated glycoprotein complex (12) and the membrane of cardiac myocytes during contractions (7). The absence of dystrophin is the primary molecular basis of Duchenne Muscular Dystrophy (DMD), a fatal X-linked neuromuscular disorder affecting 1 in 3500 live male births (11). Cardiac dysfunction is observed frequently, with cardiomyopathy shortening the lifespan of a significant proportion of boys with DMD (5, 10, 15, 16, 23). In addition to congestive heart failure, other cardiac manifestations of DMD include altered heart rate variability, arrhythmias, conduction defects and fibrosis (17). Similarly, a reduced dystrophin expression is the primary basis of congestive heart failure in X-linked cardiomyopathy and Beckers Muscular Dystrophy (6), with cardiac transplantation being undertaken as a long term treatment option.

The dystrophin deficient *mdx* mouse arose as a spontaneous mutation from a colony of C57BL10 ScSn mice, and has been widely used as an animal model of DMD for research investigating skeletal muscle dysfunction. However, the cardiovascular manifestations caused by dystrophin deficiency in the *mdx* have not been reported extensively. We have previously reported altered responsiveness to α -adrenoceptor and muscarinic receptor stimulation in young (12-14 week old) mice as well as a reduced efficacy and potency of calcium (20). In old *mdx* males (12 months), a lowered efficacy and potency of (-)-isoprenaline and reduced β_1 -adrenoceptor affinity is evident (19).

Isolated cardiac myocytes (1, 13) and skeletal muscles (31, 32) from *mdx* mice and patients with DMD (3) exhibit elevated intracellular calcium. This calcium overload can lead to decreased myocyte function and myocyte necrosis (4) resulting from calcium dependent proteolysis (30). Furthermore, *mdx* mice have been shown to exhibit dysfunctional calcium handling in both skeletal (28) and cardiac (21) myocytes. Cardiac calcium overload could potentially be due to a leaky cell membrane as postulated in skeletal muscle (31) or may result from alterations in influx or efflux, intracellular calcium handling, sarcoplasmic reticulum storage, release, sequestration or a combination of these mechanisms.

The major source of calcium influx across the cardiac cell membrane is the L-type calcium channel. This channel consists of a complex of 5 subunits, with the α_1 subunit being the channel forming, voltage-sensing component and containing the binding site for dihydropyridine (DHP) compounds such as the antagonist nifedipine and agonist Bay K 8644. This α_1 -subunit, also commonly known as the dihydropyridine receptor (DHPR), is a defining feature of cardiac L-type calcium channels and is localised within the cardiac T-tubule system, which is where dystrophin is also located (25). Thus the primary aim of this study was to examine the consequences of dystrophin deficiency on the DHPRs as a marker of L-type calcium channels regulating calcium influx.

Methods and Materials

All experimental protocols were approved by the University of Southern Queensland Animal Ethics committee under the guidelines of the National Health and Medical Research Council of Australia which conform to the National Institutes of Health Guide for the Care and Use of Laboratory Animals. Male muscular dystrophy X-linked (*mdx*) mice and their control C57BL10ScSn (C57) were used at 12-14 weeks of age. Mice were fed standard mouse chow *ad libitum* and maintained on a 12 hr light/dark cycle.

Tissue Bath Experiments

Animals were anaesthetised by excess CO₂ inhalation and euthanased by exsanguination prior to excision of their hearts. Left atria were dissected free in cold, carbogenated (95%O₂; 5%CO₂) Tyrodes physiological salt solution (TPSS in mM: NaCl 136.9, KCl 5.4, MgCl₂.H₂O 1.05, NaH₂PO₄.2H₂O 0.42, NaHCO₃ 22.6, CaCl₂.2H₂O 1.8, glucose 5.5, ascorbic acid 0.28, Na₂EDTA 0.05). A stainless steel hook was placed in one end of each atrium to connect that atrium to the tissue holder. A silk thread was tied to the other end of the atrium to connect it to a force transducer (FT-102, CB Sciences, Milford, MA, USA) to measure force of contraction. Atria were subsequently suspended in warm (35±1°C), carbogenated TPSS in tissue baths. Data were recorded via a PowerLab system (AD Instruments) using Chart 3.5.6. Left atria were field stimulated (AMPI Master 8 stimulator; 1 Hz, 5 ms duration, 20% above threshold) and maintained under optimal preload. Tissues were allowed 45 min to equilibrate with repetitive washes. At the completion of all experiments, the atria

were removed, blotted and weighed. There was no significant difference between the blotted masses of the atria taken from mdx and C57 so all force data are given as mN.

Nifedipine and Bay K 8644 Concentration Response Curves

Concentration-response curves were generated to calcium chloride to determine the maximum force of contraction attainable by the tissue. The tissues were then washed repetitively over 30 min to return the contractility to normal, and a concentration-response curve measuring the negative inotropic effects of the DHP antagonist nifedipine was generated. In order to avoid indirect receptor-mediated effects of endogenous noradrenaline possibly released by Bay K 8644, tissues were incubated with the β -adrenoceptor antagonist propranolol and α -adrenoceptor antagonist prazosin for 30min before the concentration-response curve to Bay K 8644 was generated. As Bay K 8644 is sensitive to light of wavelengths below 450nm, all handling and experiments with Bay K 8644 were carried out under protection from light. After experiments with Bay K 8644, the organ baths were cleaned with nitric acid to eliminate contamination of glassware and then flushed repeatedly with distilled water.

Radioligand Binding

Ventricular tissues were snap frozen in liquid nitrogen and stored at -70°C. For each experiment two ventricles were pooled to obtain sufficient membrane for five points on a saturation curve. Two ventricles were homogenized at 24 000 rpm by a Heidolph DIAx 600 after being thawed in Tris incubation solution (in mM: Tris HCl 50, EGTA 5, EDTA 1, MgCl₂ 4, Ascorbic Acid 1, Trizma Base 50; pH 7.4 adjusted with NaOH).

The homogenate was centrifuged at 1000g and the pellet discarded. The supernatant was centrifuged at 100 000g and the supernatant discarded. The membrane fraction was then resuspended in Tris incubation buffer and subsequently diluted to 1mg/mL protein after measuring the protein content (Biorad Protein Assay Kit). Membrane (200 μ g) was incubated with increasing concentrations of [3 H]-PN 200-110 (0.1-2nM) while non-specific binding was determined by the addition of 0.1mM nifedipine. Samples were incubated for 60 min at 35°C, and the incubation was then halted with the addition of 4mL ice-cold Tris incubation buffer. Samples were vacuum filtered over Whatman GFB filters and washed four times with ice-cold Tris wash buffer (in mM: Tris 50, pH 7.4). Filters were incubated overnight with scintillant and counted the following morning. Preliminary experiments confirmed that receptor affinity and density were not altered significantly by freezing and storing the tissues. Similarly, a series of preliminary experiments revealed that an incubation period of 60 min at 35°C and a protein concentration of 200 μ g were optimal.

RT-PCR

Animals were anaesthetised with sodium pentobarbitone and euthanased by exsanguination before the hearts were excised. The ventricles and left atria were dissected free in TPSS and placed in RNAlater™ (Ambion) RNA stabilisation reagent for storage at -20°C. RNA extraction was performed with the QIAGEN RNeasy® Mini Kit, utilising no more than 30mg of tissue per sample obtained from the apex of the left ventricle or the whole left atria. The tissue was lysed using a polytron rotor-stator homogeniser in proprietary buffer containing guanidinium thiocyanate to liberate RNA prior to the extraction procedure. RNA was isolated via binding to a

silica-gel-based membrane during a number of centrifugation procedures as per the manufacturer's instructions.

RT-PCR was performed by the two-tube method using QIAGEN OmniscriptTM Reverse Transcriptase and QIAGEN HotStarTaqTM DNA Polymerase. Tubes containing the reaction mixture were incubated in a Corbett Research PC-960C thermocycler. 0.2µM of each α 2-subunit primer (TCC AGT TTA TAC TAC TTT GGC TGG T sense; ACT GAG GGC TCA TGT TTT GG antisense) or GAPDH primer (TTA GCA CCC CTG GCC AAG G sense; CTT ACT CCT TGG AGG CCA TG antisense); and HotStarTaqTM DNA Polymerase. PCR product was visualised following gel electrophoresis by ethidium bromide staining and UV transillumination in an AlphaImager 2200 MultiImage cabinet. Spot densitometry was performed using AlphaEase and the ratio of DHPR band intensity to GAPDH band intensity was calculated for each sample to allow a semi-quantitative comparison.

Western Blotting

Total protein was extracted by homogenising frozen ventricles in lysis buffer (4% SDS, 125 mM Tris-HCl pH 6.8, 40% glycerol, 50 mM DTT) containing Protease Inhibitor Cocktail (Sigma) and 0.5 mM phenylmethylsulfonylfluoride. Proteins (60 µg) were separated on SDS-PAGE using a NuPAGE precast 4-12% Bis-Tris polyacrylamide gel and MOPS SDS running buffer (Invitrogen). After electrophoresis, proteins were transferred to a polyvinylidene difluoride membrane (Amersham). Transfer was confirmed by staining the membrane with Ponceau S stain (0.1% Ponceau S in 5% acetic acid). For detection of the α 1C subunit, the top half of

the membrane was blocked in 1x Tris-buffered saline-Tween 20 containing 5% BSA and 0.1% Tween 20. This was followed by incubation with a 1:200 dilution of anti- α_{1C} antibody (Sigma) at 4°C overnight and afterwards for 1 hour in a 1:10000 dilution of peroxidase-conjugated antibody (goat anti-rabbit polyclonal, Sigma).

For detection of α -actin, the lower half of the membrane was blocked in 1x Tris-buffered saline-Tween 20 containing 5% skim milk powder and 0.05% Tween 20. This was followed by incubation with a 1:1000 dilution of anti-actin monoclonal antibody (Clone AC-40, Sigma) at room temperature for 90 minutes and afterwards for 1 hour in a 1:6000 dilution of peroxidase-conjugated antibody (rabbit anti-mouse polyclonal, DakoCytomation). The immunoreactive bands on both western blots were visualised using ECL Plus and Hyperfilm ECL (Amersham). The western blots were analysed using Scion Image. The α_{1C} protein was normalised to α -actin to account for possible loading differences.

Patch Clamp

Animals were anaesthetised by sodium pentobarbitone (70 mg/kg) and euthanased by exsanguination prior to excision of their hearts. The aorta was cannulated and the hearts suspended on a Langendorff system for perfusion with calcium free solution (in mM: NaCl 100; KCl 5; KH₂PO₄ 1.2; MgSO₄ 5; Taurine 50; HEPES; 10; Glucose; 20; Creatine 10) at 37°C for 5 minutes followed by perfusion with collagenase type II solution (Worthington), 1% bovine zero albumin (BSA; Sigma), 0.08 mg/ml protease (Sigma) for 12 to 18 minutes. The ventricles were then removed and crudely dissociated with scissors prior to addition of cell Tyrode solution (in mM: NaCl 100; KCl 5; KH₂PO₄ 1.2; MgSO₄ 5; Taurine 50; HEPES; 10; Glucose; 20; Creatine 10) containing 0.4 mM CaCl₂. After 10 minutes, this solution was aspirated and replaced

sequentially with solution containing 0.8 and finally 1.2 mM CaCl₂ to produce calcium tolerant myocytes.

Cells were placed in a 0.5 mL perfusion chamber, allowed to settle for 5 minutes and then perfused at room temperature with oxygenated Extracellular solution (in mM: NaCl 50; MgCl₂ 3; CaCl₂ 1.8; KCl 3; TEA-Cl 90; glucose 7.7; HEPES 10; pH 7.4). Cells were patched using fire polished electrodes (1.5 – 2.5 MΩ) pulled from filamented borosilicate glass (World Precision Instruments) filled with electrode solution (in mM: CsF 135; NaCl 10; HEPES 10; EGTA 10; glucose 7.7; MgATP 2; pH 7.2). Cell recordings were obtained using a HEKA EPC-9. Cell capacitance was recorded and then cells were stepped from a holding potential of -70 mV to -40mV for 40msec to inactivate the sodium current. Cells were then stepped in 10 mV increments from -40 mV up to + 60 mV for 200 msec durations at 0.2 Hz. Initial experiments confirmed recordings of L-type calcium currents by verifying a lack of effect by 1 μM tetrodotoxin and a concentration-dependent inhibition of L-type calcium current by verapamil (1-10 μM) and cadmium (50 μM). Current density was calculated by dividing current amplitude by cell capacitance (pA/pF).

Reagents and Data Analysis

All reagents and pharmacological compounds were purchased from Sigma-Aldrich except where otherwise indicated. Data are presented as mean ± SE of the number (*n*) of experiments. Data were compared using Student's two tailed t-test and a P<0.05 was considered statistically significant.

Results

Prior to conducting the concentration-response curves to the dihydropyridines the *mdx* left atria had a lower basal force of contraction (1.50 ± 0.17 mN) compared to C57 (1.91 ± 0.18 mN; $P < 0.05$). A subsequent concentration-response curve to calcium chloride (Figure 1A) revealed increases in contractile force, however when normalized to the basal force of contraction the percentage change in both tissues was found to be similar. Of interest was the potency (EC_{50}) values calculated from this data that showed a significant difference in *mdx* when compared to C57 (*mdx* $3.40 \pm 0.08 \times 10^{-3}$ M, C57 $3.15 \pm 0.10 \times 10^{-3}$ M; $P < 0.05$)

Nifedipine reduced the force of contraction similarly in left atria from both *mdx* and C57 but was significantly less potent in left atria from *mdx* (EC_{50} values: *mdx* $3.47 \pm 0.55 \times 10^{-8}$ M; C57 $1.78 \pm 0.40 \times 10^{-8}$ M, $P < 0.05$ Fig. 1A). A strain potency ratio for nifedipine was calculated by dividing the EC_{50} of nifedipine in *mdx* by the EC_{50} of nifedipine in C57 to give a value of 1.9. Bay K 8644 elicited a strong positive inotropic effect in both strains producing a similar efficacy to calcium. Although the efficacy (as a percent of calcium chloride) was not different between the two strains, a reduced potency (EC_{50} values *mdx* $7.94 \pm 0.55 \times 10^{-7}$ M; C57 $2.95 \pm 0.34 \times 10^{-7}$ M, $P < 0.05$ Fig. 1B) was again evident in *mdx*. The strain potency ratio for Bay K 8644 was 2.7, which is similar to the ratio obtained for nifedipine. The solvent ethanol elicited a weak negative inotropic effect at the maximum solvent concentration, but this was completely overcome by the pronounced positive inotropic effect of Bay K 8644.

Radioligand binding experiments revealed a significantly greater density of DHPRs in *mdx* (Bmax 99.2±7.0 fmol/mg) compared to C57 (Bmax 74.5±9.4 fmol/mg; Fig. 2A, $P<0.05$) with a strain ratio (Bmax *mdx* /Bmax C57) of 1.3. The affinity of [³H]-PN 200-110 was also reduced significantly in *mdx* (Kd 0.3677±0.08nM) compared to C57 (Kd 0.1789±0.08nM) (Fig. 2A and B, $P<0.05$). The strain potency ratio (Kd *mdx* /Kd C57) was 2.0, a similar ratio to that observed in the functional tissue bath studies utilizing nifedipine and Bay K 8644.

To confirm the result of increased DHPR protein observed in the radioligand binding study, immunoblotting was also conducted on ventricular myocardium. Again this revealed increased DHPR protein in the *mdx* (Fig 2C). This was supported by the observation that ventricular DHPR mRNA was significantly higher ($P<0.005$) in *mdx* compared to C57 (Fig. 2D) when corrected for the amount of total mRNA by using the GAPDH samples. The strain ratio (band intensity *mdx* /band intensity C57) for ventricular mRNA was 2.3. The left atrial DHPR mRNA was also higher in *mdx* compared to C57, although this did not reach statistical significance ($P=0.07$). The strain ratio for atrial mRNA for DHPRs was 2.0. The ubiquitous β-actin was also used as a housekeeper gene (data not shown) and produced qualitatively similar data to GAPDH normalisation.

Patch clamp experiments were then conducted to determine if the increased DHPR expression resulted in a larger current amplitude. The currents were not inhibited by tetrodotoxin, but were dose-dependently inhibited by verapamil and cadmium confirming the appropriateness of the experimental conditions (data not shown). There was no significant difference in whole cell membrane capacitance (*mdx* 161±10

pF, C57 147 ± 13 pF: n=10) and no significant difference in peak current density at a test potential of 0 mV (*mdx* 4.67 ± 0.39 pA/pF, C57 5.45 ± 0.58 pA/pF). However, further analysis revealed that the time to 90% inactivation of the L-type current was increased in *mdx* myocytes compared to C57 myocytes ($P<0.05$: Fig 3).

Discussion

This study is the first to measure the properties of DHPRs in dystrophin-deficient myocardium and shows a reduced potency to both a DHPR agonist and antagonist, reflected by reduced receptor affinity, upregulation of DHPR mRNA and protein and delayed inactivation of the L-type calcium current.

Alterations in receptor regulation are a commonly observed phenomenon in cardiovascular disease states. Such alterations are generally evidenced initially by impaired potencies or efficacies to agonists which reflect changes in receptor stimulus, however, this study showed a similar difference in potency with the DHPR antagonist nifedipine. This potency difference can be explained by a lowered receptor affinity (higher K_d) as observed in the radioligand binding studies which utilised antagonists and thus are not dependent on receptor stimulus and agonist efficacy.

A possible mechanism that could affect the affinity of DHPRs is a change in the proportion of channels in the inactivated state which could be reflected by a change in the cell membrane potential, with depolarisation of the cardiac resting membrane potential causing an increase in DHPR affinity and thus presumably hyperpolarisation causing a decrease in DHPR affinity (2). However, microelectrode studies in left atria of *mdx* and C57 mice utilising the same conditions as those in the tissue bath studies did not show any difference in resting membrane potential with or without a calcium channel antagonist present (data not shown), eliminating this as a basis for the difference in DHPR affinity in the tissue bath studies. Furthermore, the difference in receptor affinity was maintained in the radioligand binding studies, where the

influence of the membrane potential is eliminated. This provides clear evidence that a change in receptor affinity is not due to changes in membrane potential.

Another influence affecting DHPR affinity is the concentration of free calcium. Using [³H]-PN 200-110 in radioligand binding studies, Peterson and Catterall (26) showed that divalent ions cause a biphasic effect on the affinity of DHPRs, with a low free calcium causing an increase in affinity, while a high free calcium causes a significant decrease in affinity. It is therefore, highly feasible that the calcium overload observed in *mdx* myocytes is a mediator responsible for the lowered affinity state of the DHPRs observed in the atrial contractility studies. However, in DHPR radioligand binding studies, calcium is not added to the incubation buffer and chelators such as EGTA are also present. This then eliminates any acute effects of calcium on modifying the affinity state of the DHPRs within such studies. Given that a lowered affinity for [³H]-PN 200-110 was still observed, this may suggest that chronic *in vivo* elevation of intracellular calcium may cause a more rigid conformational change in DHPRs, that is subsequently maintained in isolated membranes.

Alternatively, a disruption in DHPR localization due to dystrophin deficiency may be possible. DHPRs are located in the transverse tubules (T tubules) of the myocyte which is also the major site where cardiac dystrophin is located (25, 29). Furthermore, dystrophin has been suggested to play a role in anchoring or modulating the activity of cardiac DHPRs (24), among other channels (8). Therefore, the deficiency of dystrophin could result in a direct defect in the DHPR that in turn may contribute to the observed reduction of potency in *mdx* cardiac tissues and a compensatory increase in DHPRs. It is highly probable that an increase in intracellular calcium is the cause of

the elevated DHPRs as Davidoff et al (8) reported that incubation of adult rat ventricular myocytes in high extracellular calcium (4.8 mM) showed remarkably similar changes to those reported in the current study, including elevated DHPR mRNA levels 1.5 fold and DHPR density 2 fold.

Clearly, if an elevation of DHPRs is evident, then an alteration in the L-type calcium current could be expected. This current study using 12-14 week old mice showed no change in current density between *mdx* and C57 confirming previous findings by Alloatti et al (1) who utilised *mdx* mice (of an unstated age) and Sadeghi et al (27) who utilised cultured neonatal cardiac myocytes from 1 to 4 day old *mdx* mice. The basis for the lack of change in current density has not been ascertained to date and requires further investigation. Possible mechanisms could be either an uncoupling and/or mislocalisation of additional DHPR ($\alpha 1c$) subunits from the remaining L-type calcium channel subunits or an elevation in intracellular calcium reducing the driving force for calcium influx (9).

Although no change in current density was evident, a significant delay in inactivation of the L-type calcium current in adult *mdx* myocytes was observed further confirming similar findings obtained using neonatal *mdx* myocytes (27). Inactivation of L-type calcium channels is controlled by voltage and calcium-dependent mechanisms (18). A previous study utilising neonatal *mdx* myocytes using barium as the charge carrier instead of calcium, since it does not contribute effectively in mediating ion-dependent inactivation, showed that dystrophin deficiency alters L-type calcium channel inactivation by a shift in the voltage dependence of activation. The current study used calcium as the charge carrier and as such allows a contribution of calcium-dependent

inactivation mechanisms. Such inactivation will thus be affected by alterations in calcium handling proteins such as SERCA with a reduced SERCA activity having been shown to slow calcium dependent inactivation (22). The *mdx* mouse has been reported to have reduced expression of SERCA, suggesting that calcium-dependent inactivation may also be slowed in *mdx* cardiac myocytes. Finally, the lack of dystrophin may also alter calcium dependent L-type channel inactivation directly since dystrophin may bind directly to calcium channels to affect inactivation (27). The result of the delay in inactivation could be a contributor to the further development of calcium overload in *mdx* cardiac myocytes which in turn would directly affect contractility.

Distinct differences in contractility were observed with a significantly lower force of contraction from left atria of *mdx* compared to C57 mice evident prior to the addition of drugs in all of the functional experiments undertaken. This impaired capacity to generate force remained in spite of elevated extracellular calcium as previously reported (19, 20). Interestingly, the potency of calcium is also lowered when conducting a concentration-response curve to extracellular calcium. This reduction in potency to calcium and reduced capacity to generate force is indicative of a reduced sensitivity of the contractile proteins to calcium. One possible explanation for this is that chronically elevated intracellular calcium such as that observed in dystrophic muscles could cause a significant reduction in myofilament sensitivity (14).

In conclusion, dystrophin is essential for normal regulation of the L-type calcium current, DHPRs and cardiac contractility. The delayed inactivation of the L-type calcium current is a likely contributor to the elevation in intracellular calcium in the

dystrophic heart, although other mechanisms such as calcium sequestration or calcium leak from the sarcoplasmic reticulum may also be involved. The elevation in intracellular calcium is likely to contribute to the incidence of arrhythmias in DMD as well as the altered cardiac contractility.

Acknowledgements

Current address for Sai Lu is Dept Nursing and Midwifery, Victoria University, Melbourne, Victoria, 8001, Australia. Current address for Sean Holroyd is Physiology Faculty, Basic Medical Sciences (Dominica), Ross University, Edison, NJ 08837, USA.

Grants

This work was supported by funds from Parent Project Muscular Dystrophy and the Queensland Muscular Dystrophy Association.

References

1. **Alloatti G, Gallo MP, Penna C, and Levi RC.** Properties of cardiac cells from dystrophic mouse. *J Mol Cell Cardiol* 27: 1775-1779, 1995.
2. **Bean BP.** Nitrendipine block of cardiac calcium channels: high-affinity binding to the inactivated state. *Proc Natl Acad Sci U S A* 81: 6388-6392, 1984.
3. **Bertorini TE, Palmieri GM, Griffin JW, Igarashi M, McGee J, Brown R, Nutting DF, Hinton AB, and Karas JG.** Effect of chronic treatment with the calcium antagonist diltiazem in Duchenne muscular dystrophy. *Neurology* 38: 609-613, 1988.
4. **Bia BL, Cassidy PJ, Young ME, Rafael JA, Leighton B, Davies KE, Radda GK, and Clarke K.** Decreased myocardial nNOS, increased iNOS and abnormal ECGs in mouse models of Duchenne muscular dystrophy. *J Mol Cell Cardiol* 31: 1857-1862., 1999.
5. **Boland BJ, Silbert PL, Groover RV, Wollan PC, and Silverstein MD.** Skeletal, cardiac, and smooth muscle failure in Duchenne muscular dystrophy. *Pediatr Neurol* 14: 7-12, 1996.
6. **Cox GF and Kunkel LM.** Dystrophies and heart disease. *Curr Opin Cardiol* 12: 329-343, 1997.
7. **Danielou G, Comtois AS, Dudley R, Karpati G, Vincent G, Des Rosiers C, and Petrof BJ.** Dystrophin-deficient cardiomyocytes are abnormally vulnerable to mechanical stress-induced contractile failure and injury. *Faseb J* 15: 1655-1657, 2001.
8. **Davidoff AJ, Maki TM, Ellingsen O, and Marsh JD.** Expression of calcium channels in adult cardiac myocytes is regulated by calcium. *J Mol Cell Cardiol* 29: 1791-1803, 1997.

9. **Dunn JF and Radda GK.** Total ion content of skeletal and cardiac muscle in the mdx mouse dystrophy: Ca₂₊ is elevated at all ages. *J Neurol Sci* 103: 226-231, 1991.
10. **Eagle M, Baudouin SV, Chandler C, Giddings DR, Bullock R, and Bushby K.** Survival in Duchenne muscular dystrophy: improvements in life expectancy since 1967 and the impact of home nocturnal ventilation. *Neuromuscul Disord* 12: 926-929, 2002.
11. **Emery AE.** The muscular dystrophies. *Lancet* 359: 687-695., 2002.
12. **Hainsey TA, Senapati S, Kuhn DE, and Rafael JA.** Cardiomyopathic features associated with muscular dystrophy are independent of dystrophin absence in cardiovascular. *Neuromuscul Disord* 13: 294-302, 2003.
13. **Hoffman EP, Hudecki MS, Rosenberg PA, Pollina CM, and Kunkel LM.** Cell and fiber-type distribution of dystrophin. *Neuron* 1: 411-420, 1988.
14. **Holt E and Christensen G.** Transient Ca₂₊ overload alters Ca₂₊ handling in rat cardiomyocytes: effects on shortening and relaxation. *Am J Physiol* 273: H573-582, 1997.
15. **Hunsaker RH, Fulkerson PK, Barry FJ, Lewis RP, Leier CV, and Unverferth DV.** Cardiac function in Duchenne's muscular dystrophy. Results of 10-year follow-up study and noninvasive tests. *Am J Med* 73: 235-238, 1982.
16. **Hunter S.** The heart in muscular dystrophy. *Br Med Bull* 36: 133-134, 1980.
17. **Ishikawa Y, Bach JR, and Minami R.** A management trial for Duchenne cardiomyopathy. *Am J Phys Med Rehabil* 74: 345-350, 1995.
18. **Lee KS, Marban E, and Tsien RW.** Inactivation of calcium channels in mammalian heart cells: joint dependence on membrane potential and intracellular calcium. *J Physiol* 364: 395-411, 1985.

19. **Lu S and Hoey A.** Age- and sex-associated changes in cardiac beta(1)-adrenoceptors from the muscular dystrophy (mdx) mouse. *J Mol Cell Cardiol* 32: 1661-1668, 2000.
20. **Lu S and Hoey A.** Changes in function of cardiac receptors mediating the effects of the autonomic nervous system in the muscular dystrophy (MDX) mouse. *J Mol Cell Cardiol* 32: 143-152, 2000.
21. **Lucas-Heron B, Loirat MJ, Ollivier B, and Leoty C.** Calcium-related defects in cardiac and skeletal muscles of dystrophic mice. *Comp Biochem Physiol B* 86: 295-301, 1987.
22. **Masaki H, Sako H, Kadambi VJ, Sato Y, Kranias EG, and Yatani A.** Overexpression of phospholamban alters inactivation kinetics of L-type Ca²⁺ channel currents in mouse atrial myocytes. *J Mol Cell Cardiol* 30: 317-325, 1998.
23. **Melacini P, Vianello A, Villanova C, Fanin M, Miorin M, Angelini C, and Dalla Volta S.** Cardiac and respiratory involvement in advanced stage Duchenne muscular dystrophy. *Neuromuscul Disord* 6: 367-376, 1996.
24. **Meng H, Leddy JJ, Frank J, Holland P, and Tuana BS.** The association of cardiac dystrophin with myofibrils/Z-disc regions in cardiac muscle suggests a novel role in the contractile apparatus. *J Biol Chem* 271: 12364-12371, 1996.
25. **Peri V, Ajdukovic B, Holland P, and Tuana BS.** Dystrophin predominantly localizes to the transverse tubule/Z-line regions of single ventricular myocytes and exhibits distinct associations with the membrane. *Mol Cell Biochem* 130: 57-65, 1994.
26. **Peterson BZ and Catterall WA.** Calcium binding in the pore of L-type calcium channels modulates high affinity dihydropyridine binding. *J Biol Chem* 270: 18201-18204, 1995.

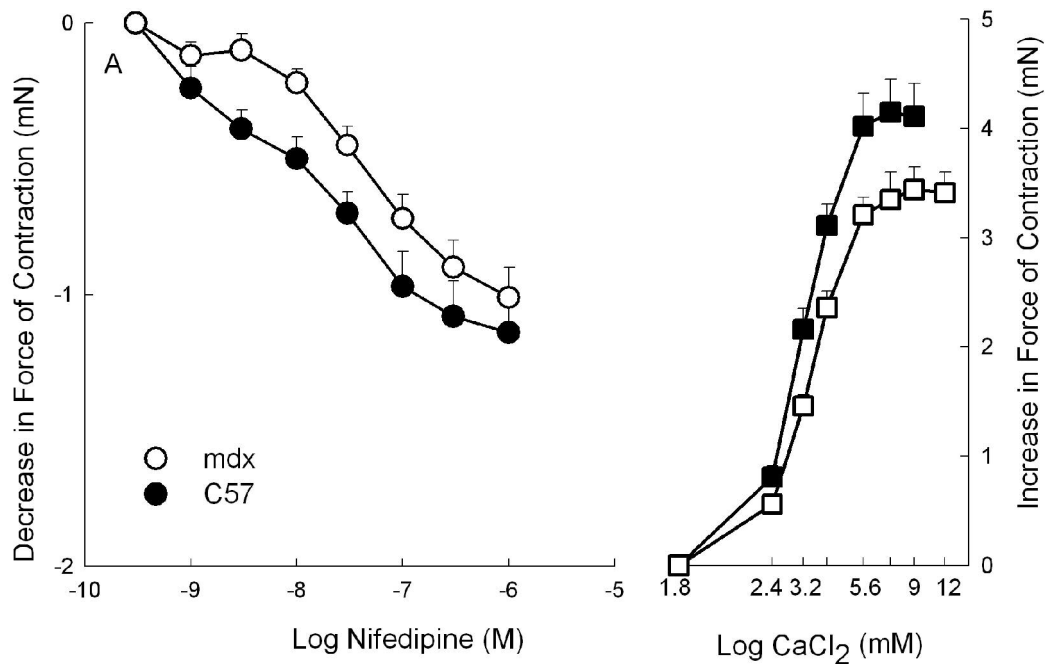
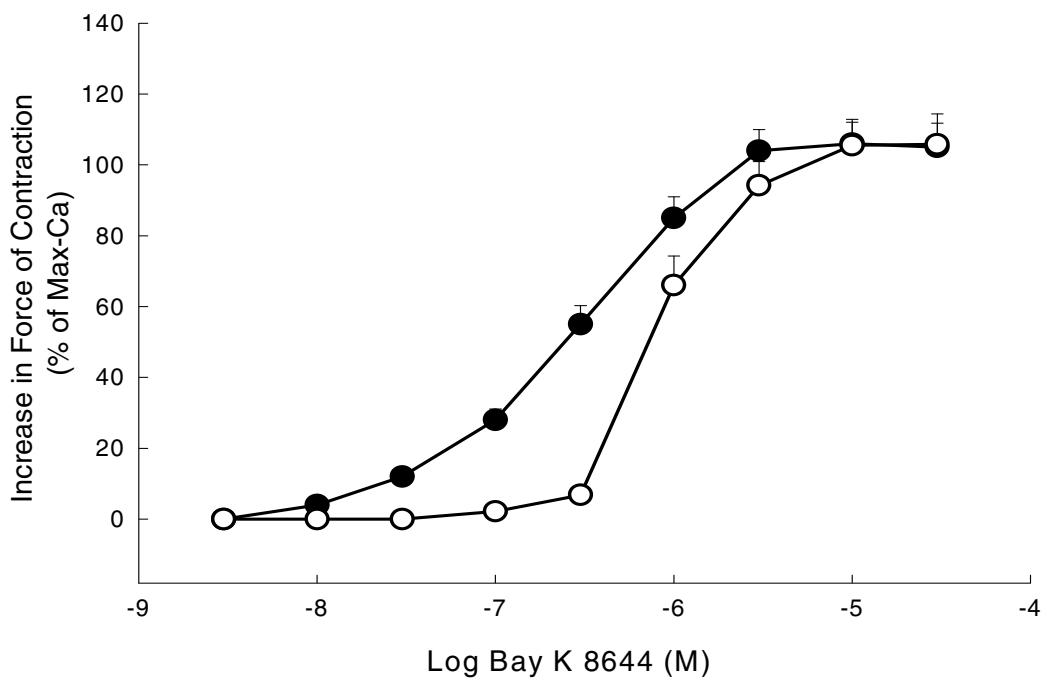
27. **Sadeghi A, Doyle AD, and Johnson BD.** Regulation of the cardiac L-type Ca₂₊ channel by the actin-binding proteins alpha-actinin and dystrophin. *Am J Physiol Cell Physiol* 282: C1502-1511, 2002.
28. **Samaha FJ and Gergely J.** Biochemical abnormalities of the sarcoplasmic reticulum in muscular dystrophy. *N Engl J Med* 280: 184-188, 1969.
29. **Takagishi Y, Yasui K, Severs NJ, and Murata Y.** Species-specific difference in distribution of voltage-gated L-type Ca(2+) channels of cardiac myocytes. *Am J Physiol Cell Physiol* 279: C1963-1969, 2000.
30. **Tidball JG and Spencer MJ.** Calpains and muscular dystrophies. *Int J Biochem Cell Biol* 32: 1-5, 2000.
31. **Turner PR, Fong PY, Denetclaw WF, and Steinhardt RA.** Increased calcium influx in dystrophic muscle. *J Cell Biol* 115: 1701-1712, 1991.
32. **Turner PR, Westwood T, Regen CM, and Steinhardt RA.** Increased protein degradation results from elevated free calcium levels found in muscle from mdx mice. *Nature* 335: 735-738, 1988.

Figure Legends

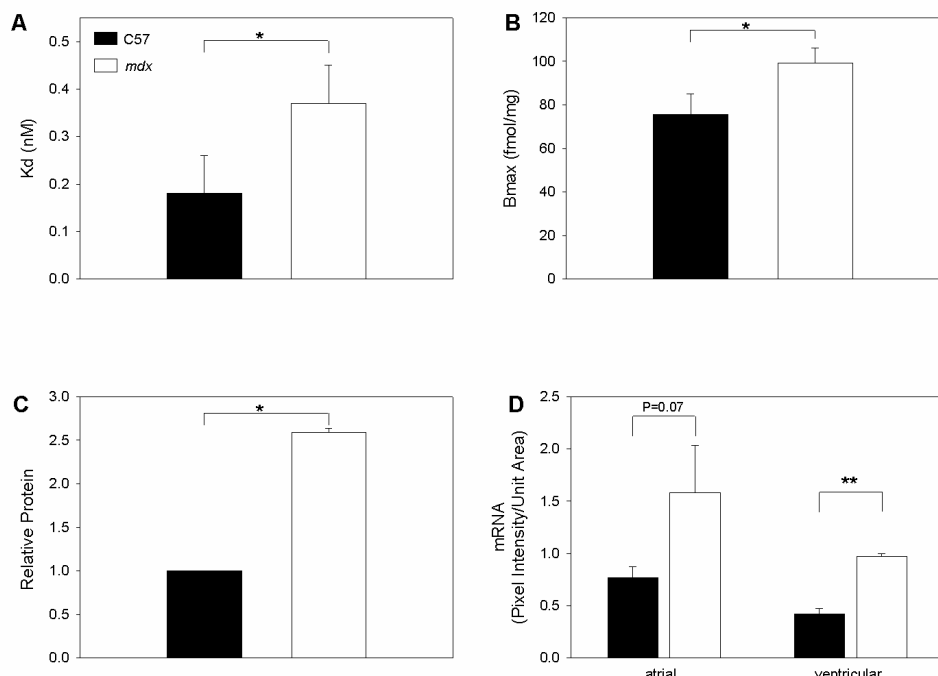
Figure 1 (A) Effect of nifedipine on left atria (n=8). EC₅₀ values for *mdx* (○) $3.47 \pm 0.55 \times 10^{-8}$ M and for C57 (●) $1.78 \pm 0.40 \times 10^{-8}$ M ($P < 0.05$). Response to increasing concentrations of extracellular calcium also shown (*mdx* (□), C57 (■) revealing a significant difference in potency and efficacy to calcium ($P < 0.01$). **(B)** Responses to Bay K 8644 in isolated *mdx* (○) and C57 (●) atria. Concentration-response curve to Bay K 8644 in left atria (n=8). EC₅₀ values for *mdx* $7.94 \pm 0.55 \times 10^{-7}$ M and for C57 $2.95 \pm 0.34 \times 10^{-7}$ M ($P < 0.05$). See text for basal forces recorded at 1.8 mM calcium.

Figure 2 (A and B) Radioligand binding experiments from *mdx* (open: n= 15 experiments; 30 ventricles) and C57 (filled: n = 19 experiments; 38 ventricles) in response to increasing concentrations of [³H]-PN 200-110 (0.1-2nM). Non-specific binding was determined by the addition of 0.1M nifedipine. There is a significant difference between *mdx* and C57 for both K_d (**2A**) and B_{max} (**2B**) ($P < 0.05$). **(C)** Normalised data from Western blots of *mdx* and C57 ventricles showing evidence of increased DHPR protein in the *mdx* ventricles (n=3). **(D)** RT-PCR results from *mdx* and C57 dihydropyridine receptor mRNA from ventricles and left atria (n=4). Band intensity was normalised to the amount of mRNA present by comparing each DHPR sample to its corresponding GAPDH sample. Ventricular mRNA was significantly higher in *mdx* ($P < 0.005$) compared to C57. * indicates $P < 0.05$. ** indicates $P < 0.01$.

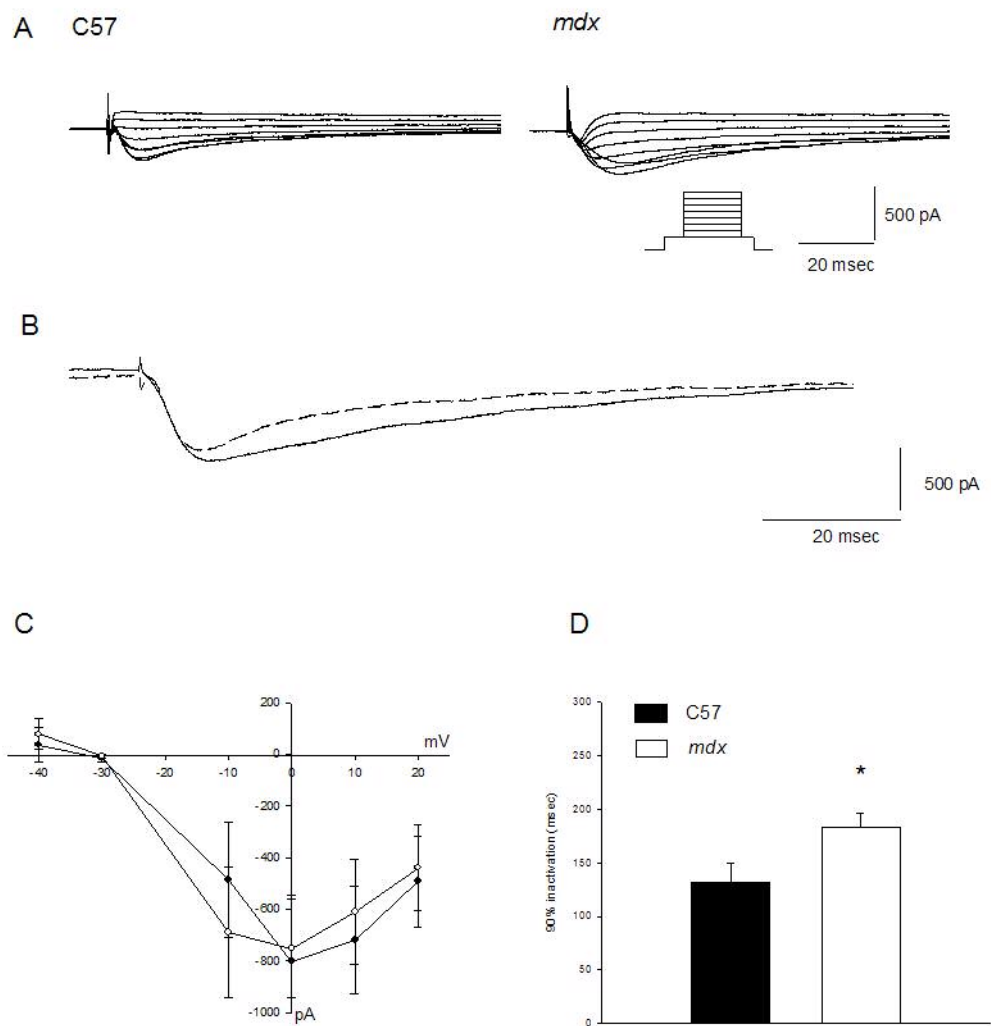
Figure 3. Calcium currents from *mdx* and C57 myocytes (n=10). **(A)** Original recordings of I-V traces for calcium currents from *mdx* and C57 cardiac myocytes indicating similar current amplitude. **(B)** Original recording of a calcium current from *mdx* (solid) and C57 (dashed) cardiac myocytes revealing the delay of inactivation in the *mdx* myocyte. **(C)** I_{Ca} -V relationships from *mdx* and C57 cardiac myocytes showing no significant differences in shapes of the curves. (*mdx* open, C57 filled) **(D)** Time to 90% inactivation showing a significant increase in inactivation time in *mdx* myocytes. (*mdx* open, C57 filled) * indicates $P<0.05$.

A**B**

Woolf et al Figure 1



Woolf et al Figure 2



+

Woolf et al Figure 3